

Probing the Boundaries between Lewis-Basic and Redox Behavior of a Parent Borylene

Merle Arrowsmith,^[a, b] Sara Endres,^[a, b] Myron Heinz,^[c] Vincent Nestler,^[a, b]
Max C. Holthausen,^[c] and Holger Braunschweig^{*[a, b]}

Abstract: The parent borylene (CAAC)(Me₃P)BH, **1** (CAAC = cyclic alkyl(amino)carbene), acts both as a Lewis base and one-electron reducing agent towards group 13 trichlorides (ECl₃, E = B, Al, Ga, In), yielding the adducts **1-ECl₃** and increasing proportions of the radical cation [**1**]^{•+} for the heavier group 13 analogues. With boron trihalides (BX₃, X = F, Cl, Br, I) **1** undergoes sequential adduct formation and halide

abstraction reactions to yield borylboronium cations and shows an increasing tendency towards redox processes for the heavier halides. Calculations confirm that **1** acts as a strong Lewis base towards EX₃ and show a marked increase in the B–E bond dissociation energies down both group 13 and the halide group.

Introduction

With their formal lone pair at boron, boryl anions and borylenes are strong boron-based nucleophiles, while their formally empty p orbital(s) also make them highly electrophilic (Figure 1). Since the isolation of the first boryl anion, [I][−], by Yamashita in 2006^[1] and the first metal-free doubly base-stabilized borylene, **II**, by Bertrand in 2010^[2] (Figure 2) significant progress has been made in the targeted synthesis and the exploration of the reactivity of these unusually electron-rich boron(II) compounds.

The nucleophilic character of boryl anions and borylenes towards main group Lewis acids can be exploited, in particular to generate new bonds between boron and elements of group 13 (E = B, Al, Ga, In). Yamashita's boryl anion, for example, coordinates as an anionic donor to BH₃ and EMe₃ (E = Al, Ga) to yield the corresponding borylborates, [I-BH₃][−],^[4] and [I-EMe₃][−],^[5]

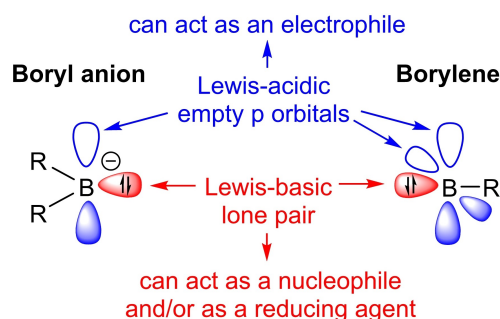


Figure 1. Schematic representation of the electronic structure of boryl anions and borylenes.

respectively (Figure 2a). In the presence of additional EMe₃, however, methyllithium is abstracted from [Li(thf)₂][I-EMe₃] to yield the neutral species I-EMe₂(thf) and the ionic by-product, Li[EMe₄] (Figure 2b).^[5,6] THF can then be abstracted from I-EMe₂(thf) either *in vacuo* or by adding further EMe₃ as a Lewis acidic THF scavenger. With group 13 trihalides, [I][−] systematically undergoes either single or double salt metathesis to yield the neutral dinuclear species I-E(X)₂(thf) (Figure 2c)^[7] or the trinuclear species I-E(X)-I (Figure 2d),^[7,8] which display electron-sharing covalent B–E bonds. Similarly, an unsaturated analogue of [I][−] undergoes salt metathesis with B(OMe)₃ to yield the corresponding unsymmetrical 1,1-dialkoxy-2,2-diaminodiborane (**4**).^[9]

The reactivity of borylenes towards group 13 trihalides has not been so widely explored. Whereas Bertrand's hydroborylene **II** undergoes a one-electron oxidation with GaCl₃ to yield the corresponding boryl radical cation, [II]^{•+} (Figure 2e),^[2] our group and that of Kinjo have shown that the doubly base-stabilized arylborylenes **III** and **IV** react with gallium trihalides to form the Lewis adducts **III-GaX₃** (Figure 2f)^[10] and **IV-GaCl₃** (Figure 2g),^[11] respectively. From these reactions it becomes apparent that

[a] Dr. M. Arrowsmith, S. Endres, V. Nestler, Prof. Dr. H. Braunschweig
Institute for Inorganic Chemistry
Julius-Maximilians-Universität Würzburg
Am Hubland, 97074 Würzburg
(Germany)
E-mail: h.braunschweig@uni-wuerzburg.de

[b] Dr. M. Arrowsmith, S. Endres, V. Nestler, Prof. Dr. H. Braunschweig
Institute for Sustainable Chemistry & Catalysis with Boron
Julius-Maximilians-Universität Würzburg
Am Hubland, 97074 Würzburg
(Germany)

[c] M. Heinz, Prof. Dr. M. C. Holthausen
Institut für Anorganische und Analytische Chemie
Goethe-Universität Frankfurt am Main
Max-von-Laue-Str. 7, 60438
Frankfurt am Main (Germany)

Supporting information for this article is available on the WWW under
<https://doi.org/10.1002/chem.202103256>

© 2021 The Authors. Chemistry - A European Journal published by Wiley-VCH GmbH. This is an open access article under the terms of the Creative Commons Attribution License, which permits use, distribution and reproduction in any medium, provided the original work is properly cited.

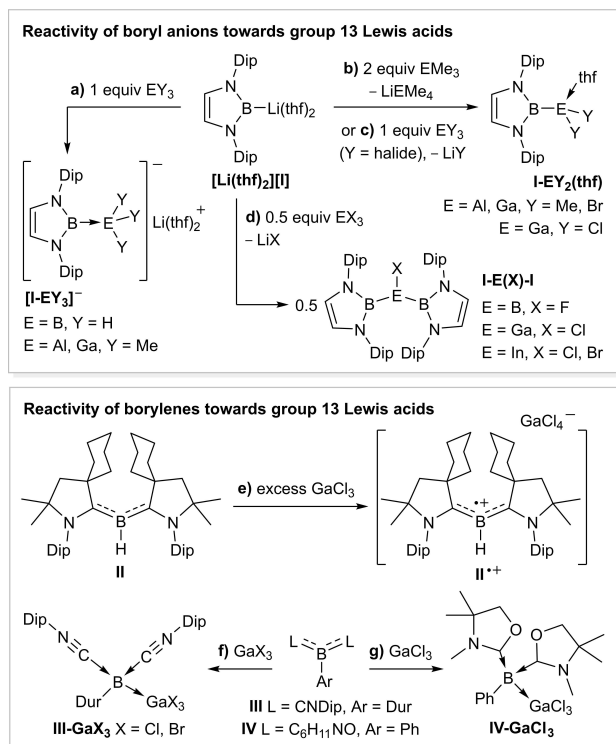


Figure 2. Reported reactivity of boryl anions and borylenes towards group 13 Lewis acids. Dip = 2,6-*i*-Pr₂C₆H₃; Dur = 2,3,5,6-Me₄C₆H₂.

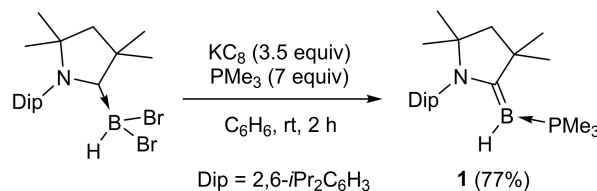
boron(I) species can interact with group 13 electrophiles both as bases, forming simple adducts, or as reducing agents.

To date, however, there has been no systematic study of Lewis-basic versus redox reactivity of boron(I) compounds. In this work we present a highly reactive phosphine-stabilized parent borylene and systematically investigate its reactivity towards the series of group 13 trichlorides (ECl₃, E = B, Al, Ga, In) and of boron trihalides (BX₃, X = F, Cl, Br, I). We show that trends in the selectivity of these reactions for either Lewis adduct formation and/or redox chemistry can be correlated to both the nature of the group 13 element and that of the halide. Computational investigations provide insights into the nature of the B–E bond in a series of borylene-EX₃ adducts.

Results and Discussion

Synthesis of borylene 1

The room-temperature reduction of (CAAC)BHBr₂ with 3.5 equiv. KC₈ in benzene in the presence of 7 equiv. PMe₃ yielded, after workup, the mixed-base-stabilized hydroborylene (CAAC)(Me₃P)BH (1) as a yellow crystalline solid in good yield (77%, Scheme 1). The ¹¹B NMR spectrum of 1 presents an apparent triplet at –7.6 ppm, resulting from coupling to both the ¹H and ³¹P nuclei (¹J_{11B-31P} ≈ ¹J_{11B-1H} ≈ 127 Hz). The ¹¹B NMR shift of 1 is between that of the related cyanoborylene (CAAC)(PET₃)B(CN) ($\delta_{11B} = -17.8$ ppm)^[12] and chloroborylene (CAAC)(PET₃)BCl



Scheme 1. Synthesis of hydroborylene 1.

($\delta_{11B} = 5.6$ ppm).^[13] The corresponding ¹H{¹¹B} NMR BH resonance appears as a doublet at 1.72 (²J_{1H-31P} = 19.8 Hz), while the ³¹P{¹H} NMR spectrum displays a broad multiplet centered at –25.4 ppm.

The solid-state structure of 1 (Figure 3a) shows a trigonal planar borylene center ($\Sigma(\angle B1) 359.93(12)^\circ$) bound to the CAAC ligand by a planar B=C double bond (B1–C1 1.454(3) Å; torsion angles N1–C1–B1–H1 0.5(14)°, N1–C1–B1–P1 179.54(14)°), similar to that in (CAAC)(PET₃)BCl (1.456(3) Å), and to the phosphine by a typical B–P single bond (1.871(2) Å). While a number of CAAC-stabilized parent borylenes have been reported,^[2,14] this is the first phosphine-stabilized example and the one presenting the least steric congestion at the borylene center, making it likely highly reactive. It therefore came as a surprise that 1 proved indefinitely stable in hydrocarbon solutions up to 100 °C and could be further purified without notable decomposition from traces of the hydrolysis by-product (CAAC)BH₃ by sublimation (110 °C, 10³ mbar). Density functional theory (DFT) calculations at the RI-DSD-BLYP-D3BJ/def2-QZVPP//PBEh-3c level of theory (see Supporting Information for details) show that the HOMO, which represents the formal lone pair at boron, is slightly delocalized over the B–C π bond (B: 35%, C: 21%, see Table S6 in the Supporting Information) with a small antibonding contribution of the CAAC nitrogen p orbital (Figure 3b), similar to other (CAAC,PR₃)-stabilized borylenes.^[12,13] Natural population analysis (NPA) provides a calculated charge at boron of –0.40 (see legend of Figure 3), suggesting that 1 should be a strong boron-centered nucleophile. Furthermore, the relatively small size of the hydride and PMe₃ ligands afford sufficient space in

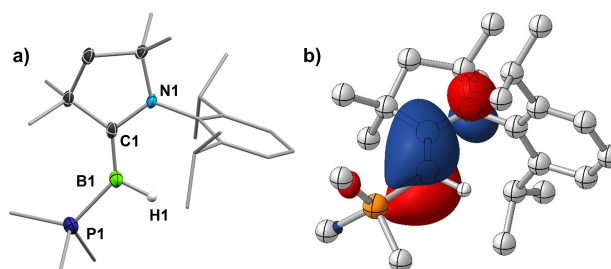
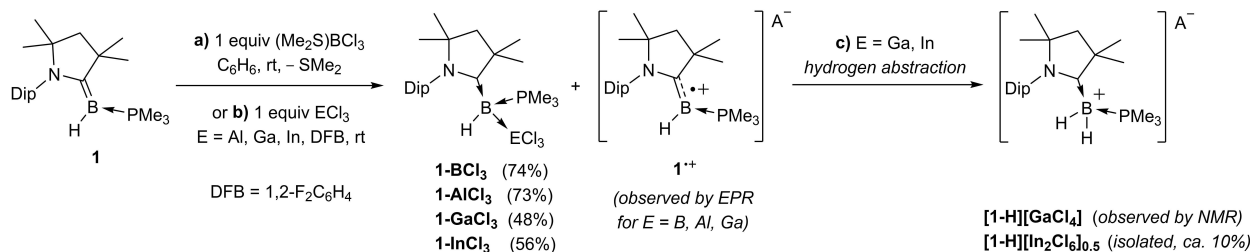


Figure 3. a) Crystallographically-derived molecular structure of 1. Atomic displacement ellipsoids drawn at 50% probability level. Ellipsoids on ligand periphery and hydrogen atoms omitted for clarity. b) Plot of the HOMO of 1 (RI-DSD-BLYP-D3BJ/def2-QZVPP//PBEh-3c level, isovalues $\pm 0.05 a_0^{-3/2}$). PBEh-3c-NPA charges: B1 –0.40, H1 0.00, C1 –0.08, N1 –0.56, P1 1.23.

Scheme 2. 1:1 reactions between **1** and group 13 trichlorides.

the coordination sphere of boron for the coordination of Lewis acids.

Synthesis and NMR-spectroscopic characterization of adducts with group 13 trichlorides

We therefore set out to investigate the adduct formation of **1** with Lewis acidic group 13 trihalides. The room-temperature reaction of borylene **1** with one equiv. (Me₂S)BCl₃ in benzene resulted in the crystallization of the colorless borylene-borane adduct **1-BCl₃** in 74% yield over the course of 30 min at room temperature (Scheme 2a).^[15] The ¹¹B NMR spectrum of **1-BCl₃** displays two broad resonances at 11.4 and -21.4 ppm corresponding to the BCl₃ and borylene moieties, respectively (Table 1). Given that the ¹¹B NMR shift of Lewis base adducts of boranes is dependent on the overall electron-donor strength of the Lewis base, a comparison with the ¹¹B NMR shifts of literature-known donor complexes of BCl₃ (Figure 4)^[16] shows that borylene **1** is a comparatively weak Lewis base, similar to dimethyl ether and dimethyl sulfide. The ³¹P NMR shift of **1-BCl₃** at -10.9 ppm is significantly downfield-shifted from that of **1**

Sample	δ _{11B} [ppm]	δ _{31P} [ppm]
1	-7.6 (t, ¹ J _{HB} ≈ ¹ J _{PB} ≈ 127 Hz)	-25.4 (m)
1-BCl₃	13.4 (br, BCl ₃), -21.4 (br, BH)	-10.9 (m)
1-AlCl₃	-26.2 (br)	-12.9 (m)
1-GaCl₃	-25.2 (br t, ¹ J _{HB} ≈ ¹ J _{PB} ≈ 81 Hz)	-11.6 (m)
1-InCl₃	-24.6 (br t, ¹ J _{HB} ≈ ¹ J _{PB} ≈ 96 Hz)	-12.4 (m)

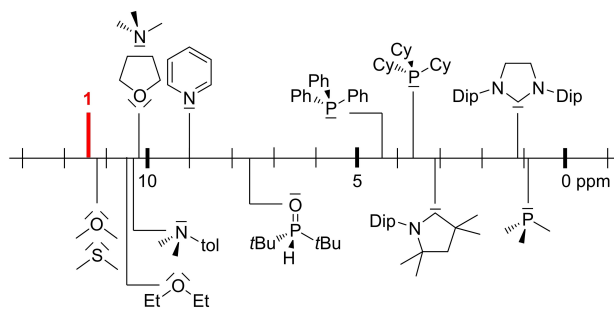


Figure 4. Comparison of the ¹¹B NMR shift of **1-BCl₃** with literature-known Lewis base adducts of BCl₃ (tol = 4-MeC₆H₄).

(δ_{11B} = -25.4 ppm), and comparable to that of the [(CAAC)(PMe₃)BH₂]⁺ cation, **[1-H]⁺** (δ_{31P} = -10.6 ppm).^[17] In the ¹H{¹¹B} NMR spectrum the BH resonance appears at 1.80 ppm as a broad doublet coupling to the neighboring phosphorus nucleus (²J_{H-31P} = 12.3 Hz), while the CAAC ligand resonances are all split due to the presence of the chiral borylene center and the hindered rotation around the B-C_{CAAC} bond.

Similarly, the 1:1 reaction between **1** and AlCl₃ in *o*-difluorobenzene (DFB) afforded the borylene-alane adduct **1-AlCl₃** as a colourless solid in 73% yield (Scheme 2b). **1-AlCl₃** shows a broad ¹¹B NMR resonance at -26.2 ppm, 5 ppm upfield of the borylene resonance of **1-BCl₃**, a ³¹P NMR multiplet at -12.9 ppm and a very broad ²⁷Al NMR resonance at 125 ppm (fwmh ≈ 1400 Hz), in the region of four-coordinate aluminium chlorides.^[18] While the 1:1 reactions with the heavier group 13 trichlorides, GaCl₃ and InCl₃, also resulted in the formation of the corresponding borylene-gallane and -indane adducts (**1-GaCl₃**; δ_{11B} = -25.2 ppm; **1-InCl₃**; δ_{11B} = -24.6 ppm), these proved less selective (Scheme 2b).^[19] In both cases the NMR spectra of the reaction mixture showed the formation of varying amounts of the known **[1-H]⁺** cation.^[17,20] For the InCl₃-based reaction single-crystal X-ray diffraction analysis confirmed the formation of the by-product **[1-H][In₂Cl₆]_{0.5}** (see Figure S41 in the Supporting Information).^[21] The formation of **[1-H]⁺** and the In₂Cl₆²⁻ counteranion, in which the indium centers are formally in the +2 oxidation state, points to a redox reaction between **1** and InCl₃, followed by hydrogen radical abstraction by the **1^{•+}** radical cation (Scheme 2c). Indeed EPR spectra of the 1:1 reactions of **1** with (Me₂S)BCl₃, AlCl₃ and GaCl₃, all showed the presence of the same radical species, presumably **[1][ECl₄]** (E = B, Al, Ga),^[22] analogous to the radical cation obtained by Bertrand from the one-electron oxidation of **II** with GaCl₃ (Figure 2e).^[2]

Isolation of the boryl radical cation **1^{•+}**

The cyclic voltammogram of **1** in THF (0.1 M [*n*Bu₄N][PF₆]) shows a reversible oxidation wave at E_{1/2} = -1.15 V and an irreversible one at E_{pa} = +0.06 V (versus Fc/Fc⁺, Fc = (C₅H₅)₂Fe, the former suggesting that a selective one-electron chemical oxidation should be achievable. A comparison with commonly used organometallic reducing agents^[23] and other mono- and dinuclear boron(I) compounds (Figure 5)^[2,12,24] shows that borylene **1** is a relatively mild one-electron reducing agent, on a

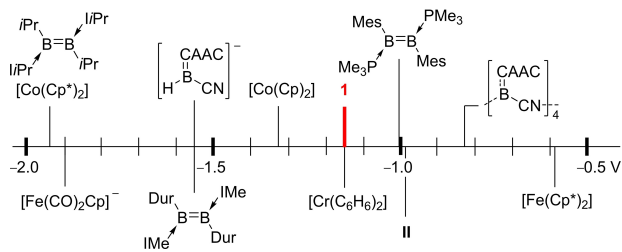
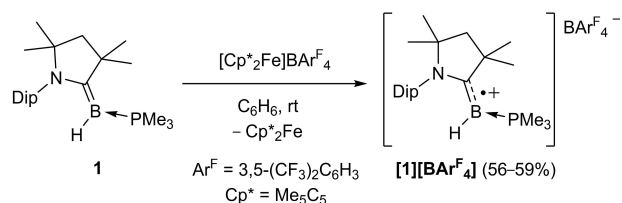


Figure 5. Comparison of the formal one-electron oxidation potential of **1** (vs. Fc/Fc⁺, Fc=Cp₂Fe) with selected organometallic reducing agents and other boron(I) compounds. Cp=C₅H₅; Cp^{*}=C₅Me₅; Dur=2,3,5,6-Me₄C₆H₂; Mes=2,4,6-Me₃C₆H₃; *i*Pr=1,3-diisopropylimidazol-2-ylidene.

par with [Cr(C₆H₆)₂] ($E_{1/2} = -1.15$ V), but is significantly more reducing than borylene **II** ($E_{1/2} = -0.94$ V)^[2] or our tetrameric cyanoborylene ($E_{1/2} = -0.83$ V).^[12]

In order to confirm the formation of **1**^{•+} in the reactions presented in Scheme 2, compound **1** was oxidized with



Scheme 3. Independent synthesis of the boryl radical cation **1**^{•+}.

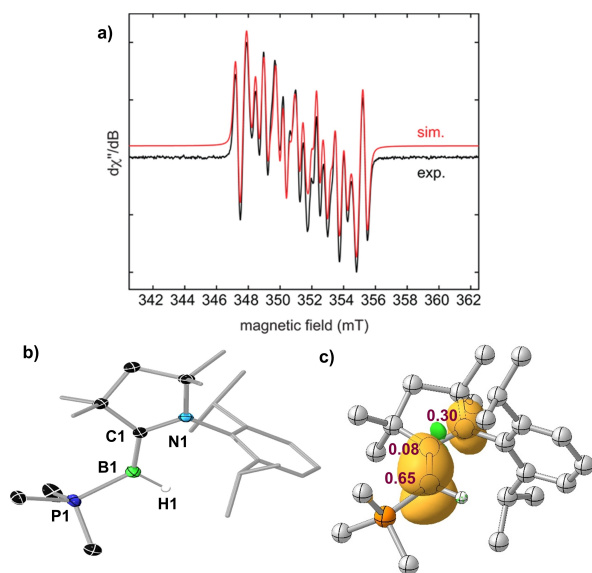


Figure 6. a) Experimental (black) and simulated (red) EPR spectrum of **1**^{•+}. b) Crystallographically-derived molecular structure of **1**^{•+} (BARF₄⁻ omitted for clarity). Thermal ellipsoids set at 50% probability. Thermal ellipsoids of ligand periphery and hydrogen atoms omitted for clarity, except for boron-bound H1. c) Plot of spin density of **1**^{•+} with Mulliken atomic spin densities at the RI-DSD-BLYP-D3BJ/def2-QZVPP//PBEh-3c level of theory (isovalues ± 0.005 a₀⁻³). PBEh-3c-NPA charges: B1 -0.01, H1 -0.01, C1 0.03, N1 -0.40, P1 1.20.

[Cp^{*}₂Fe][BAR^F₄] (Cp^{*}=C₅Me₅; Ar^F=3,5-bis(trifluoromethyl) phenyl, Scheme 3).^[25] [**1**][BAR^F₄] was isolated as highly air- and moisture-sensitive pale yellow crystals, the EPR spectrum of which was essentially identical to those recorded for the reactions shown in Scheme 2 (Figure 6a, see Figure S37 in the Supporting Information). The signal is unusually broad, spanning 105 G, and shows a unique splitting pattern. Simulation provides very large hyperfine coupling constants to the phosphorus and nitrogen nuclei ($a(^{31}\text{P}) = 29.4$ G; $a(^{14}\text{N}) = 18.1$ G; cf. **II**^{•+}: $a(^{14}\text{N}) = 4.470$ G),^[2] and coupling constants to the boron-bound hydride ($a(^1\text{H}) = 11.5$ G) and boron nucleus ($a(^{11}\text{B}) = 8.7$ G), similar to those observed in **II**^{•+} ($a(^1\text{H}) = 11.447$ G, $a(^{11}\text{B}) = 6.432$ G).^[2] The solid-state structure of **1**^{•+} shows a conformation analogous to **1** (Figure 6b), with a trigonal planar boron center ($\sum \angle_{\text{B1}} = 359.88(11)^\circ$), but significant elongation of the B1–C1 (1.508(2) Å) and shortening of the C1–N1 bonds (1.338(2) Å) compared to those **1** (B1–C1 1.454(3); C1–N1 1.408(2) Å), as expected upon oxidation. The B=C double bond remains planar as seen in the N1–C1–B1–H1 and N1–C1–B1–P1 torsion angles of 3.3(14) and 177.79(14), respectively. The NPA charge of -0.01 at boron is significantly less negative than that in **1** (-0.40), which is in line with the increase in oxidation state from +1 to +2. Furthermore, calculations show that the unpaired electron is delocalized over the B1–C1–N1 π system, with the majority of the Mulliken spin density (65%) concentrated at boron and 30% at the CAAC nitrogen atom. Among CAAC-stabilized boron radicals this is the highest spin density at boron reported to date.^[26]

Structural analyses of borylene-ECl₃ adducts

X-ray crystallographic analyses were performed on all four **1**-ECl₃ adducts (E = Al, Figure 7; E = B, Ga, In, see Figures S38–S40 in the Supporting Information). Relevant bond lengths and angles are listed in Table 2. All four compounds display a similar conformation, in which the B1-bound hydride is oriented so as to minimize the (H1–B1–C1–N1) torsion angle (13 to 21°) and thereby the steric interaction between the Dip substituent and the B1-bound PMe₃ and ECl₃ ligands. The B1–C1 (1.567(3) to 1.599(4) Å) and C1–N1 bond lengths (ca. 1.32 Å) denote B–C single and C–N double bonds, indicating that the CAAC ligand acts as a pure σ donor. The B–B bond length of 1.784(4) Å in **1**-

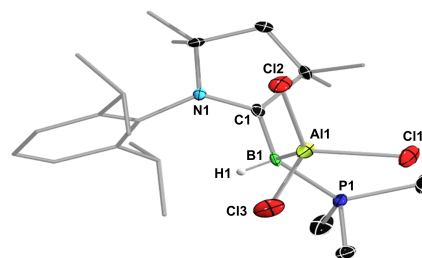


Figure 7. Crystallographically-derived molecular structure of **1**-AlCl₃. Thermal ellipsoids set at 50% probability. Thermal ellipsoids of ligand periphery and hydrogen atoms omitted for clarity, except for boron-bound H1.

Table 2. Selected bond lengths [Å] and angles [°] of crystallographically characterized compounds.								
	1-BCl ₃ ^[a]	1-AlCl ₃ ^[b]	1-GaCl ₃ ^[c]	1-InCl ₃ ^[d]	[1-BF ₂][BF ₄] ^[a,e]	[1-BCl ₂][BCl ₄] ^[a]	4 ^[a]	[1-I]
B1–C1	1.599(4)	1.567(3)	1.592(2)	1.579(2)	1.588(6), 1.602(6)	1.609(4)	1.620(4)	1.607(6)
B1–H1	1.14(3)	1.06(2)	1.06(2)	1.07(2)	1.18(5), 1.07(5)	1.12(4)	1.16(3)	1.12(5)
B1–P1	1.969(3)	1.927(2)	1.951(2)	1.939(2)	1.959(5), 1.942(5)	1.963(3)	1.974(4) ^[f]	1.977(5)
B1–E	1.784(4)	2.191(2)	2.153(2)	2.314(2)	1.733(7), 1.719(7)	1.709(4)	1.736(5)	2.290(5) ^[g]
N1–C1	1.318(3)	1.322(2)	1.320(2)	1.313(2)	1.305(5), 1.298(5)	1.313(4)	1.308(4)	1.305(6)
Torsion (H1-B1-C1-N1)	21(1)	13(1)	15(1)	13(1)	17(3), 22(3)	22(2)	7(2)	–

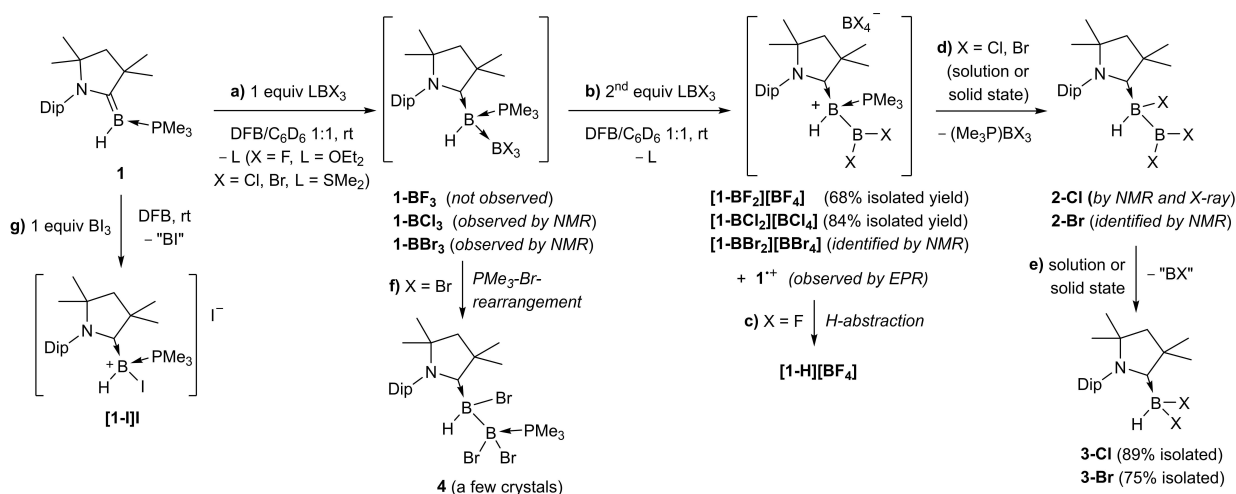
[a] E = B. [b] E = Al. [c] E = Ga. [d] E = In. [e] Two crystallographically distinct molecules in the asymmetric unit. [f] B2–P1. [g] E = I.

BCl₃ is similar to that of 1.797(4) Å in a bis(phosphine)-stabilized borylene-borane recently reported by our group.^[27] Complex 1-AlCl₃ is only the third borylene-alane reported to date, its B–Al bond length of 2.191(2) Å being identical to that of our recently reported aminoborylene-alane adduct (2.196(4) Å).^[28] The B–Ga bond length of 2.153(2) Å is only slightly shorter than that reported for III-GaCl₃ and IV-GaX₃ (ca. 2.17 Å).^[10,11] Complex 1-InCl₃ (B–In 2.314(2) Å) is, to our knowledge, the first reported borylene-indane complex. It is noteworthy that the B–E bond lengths do not increase linearly down the group. Indeed the B–Al bond in 1-AlCl₃ (2.191(2) Å) is slightly longer than the B–Ga bond in 1-GaCl₃ (2.153(2) Å). This inverse trend has been observed previously in I-EMe₂(thf) (Figure 2b), in which the B–Al bonds (ca. 2.15 Å) are significantly longer than the B–Ga bonds (ca. 2.07 Å) owing to the d-orbital contraction in gallium. This is also apparent in the quasi identical covalent radii of Al ($r = 1.21(4)$ Å) and Ga ($r = 1.22(3)$ Å).^[29]

Reactivity of borylene 1 towards boron trihalides

Having determined these trends in the reactivity of ECl₃ with borylene 1 (E = B, Al, Ga, In), we studied variations of the halide to identify further trends. Independent of the reaction conditions, combining 1 with (Et₂O)BF₃ resulted in a rapid 1:2 reaction,^[30] forming [1-BF₂][BF₄] as the major product (ca. 80%) and [1-H][BF₄] as the sole NMR-active by-product (Scheme 4a–c). Furthermore, the radical species 1^{•+} was detected by EPR spectroscopy. The formation of [1-BF₂][BF₄] can be rationalized by fluoride ion abstraction from an initial 1-BF₃ adduct by a second BF₃ equivalent (Scheme 4a,b). The fact that 1-BF₃ was never observed implies that fluoride abstraction occurs significantly faster than adduct formation in this case, presumably due to the much lower Lewis acidity of BF₃ compared to BCl₃^[31] and its high fluoride ion affinity.^[32]

The ¹¹B NMR spectrum of [1-BF₂][BF₄] shows two broad resonances at 34.6 (sp²-B) and –30.8 (sp³-B) ppm for the diboron cation and a sharp singlet at 0.1 ppm for the [BF₄][–] anion. The ¹⁹F NMR spectrum displays two singlets at –38.5 and –138.7 for the BF₂ moiety and the [BF₄][–] anion, respectively. The solid-state structure of [1-BF₂][BF₄] (Figure 8, Table 2) shows



Scheme 4. Divergent reactivity of 1 towards BX₃ (X = F, Cl, Br, I).

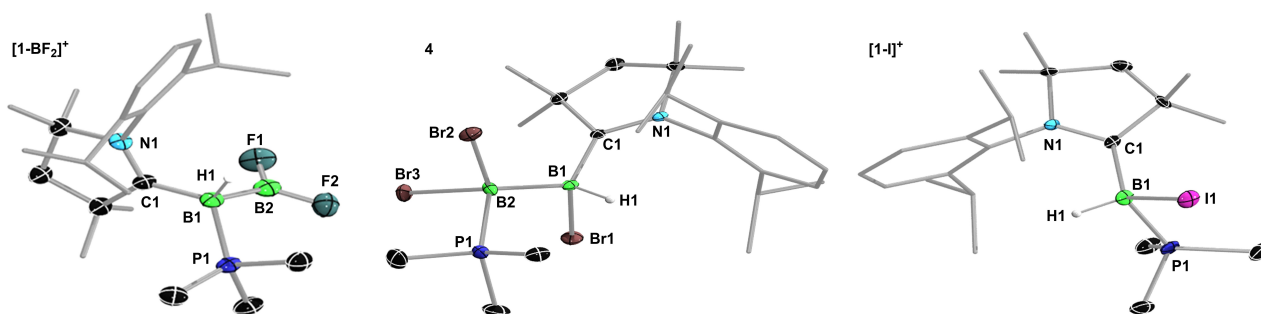


Figure 8. Crystallographically-derived molecular structures of $[1\text{-BF}_2]^+$ (one of the two cations present in the asymmetric units), **4** and $[1\text{-I}]^+$. Thermal ellipsoids set at 50% probability. Thermal ellipsoids of ligand periphery, the BF_4^- counteranion of $[1\text{-BF}_2]^+$, the iodide counteranion of $[1\text{-I}]^+$ and hydrogen atoms omitted for clarity, except for boron-bound H1.

a sp^2 -hybridized B2 center ($\Sigma\angle_{\text{B2}} \approx 360^\circ$),^[33] with C1, B1, B2, F1 and F2 all belonging to the same plane (torsion angle (C1–B1–B2–F1) ca. 10°). The B–B bond (avg. 1.726 Å) is similar in length to those of other structurally characterized doubly base-stabilized $\text{sp}^2\text{-sp}^3$ borylboronium cations (avg. 1.73 Å).^[34]

Independent of the reaction conditions the reaction of **1** with $(\text{Me}_2\text{S})\text{BBr}_3$ or BBr_3 proved highly unselective.^[35] While the formation of **1-BBr₃** ($\delta_{11\text{B}} = -4.9$ (br, BBr_3), -20.1 (br, BH); $\delta_{31\text{P}} = -12.1$ (m) ppm, Scheme 4a) was observed when working with substoichiometric amounts of BBr_3 at -70°C , this adduct could not be isolated cleanly.^[36] As with $(\text{Et}_2\text{O})\text{BF}_3$ the room temperature reaction always consumed two equiv. BBr_3 and also resulted in a complex mixture of at least five boron-containing species. Over the course of one day at room temperature, however, this mixture resolved into two major products, formed in a 1:1 ratio: $(\text{Me}_3\text{P})\text{BBr}_3$ ($\delta_{11\text{B}} = -4.4$ (d, $J_{11\text{B}-31\text{P}} = 150$ Hz) ppm; $\delta_{31\text{P}} = -7.9$ (m) ppm) and the known compound $(\text{CAAC})\text{BHBr}_2$, **3-Br** (Scheme 4e).^[37] In order to elucidate the mechanism of this reaction, our attention turned to the analogous 1:2 reaction between **1** and $(\text{Me}_2\text{S})\text{BCl}_3$. Carried out in a 1:1 DFB/benzene mixture, it resulted in the instant precipitation of $[1\text{-BCl}_2][\text{BCl}_4]$ ($\delta_{11\text{B}} = 75.8$ (br, BCl_2), 8.3 (s, BCl_4^-), -23.5 (br, BH) ppm; Scheme 4a,b). The solid-state structure of $[1\text{-BCl}_2][\text{BCl}_4]$ (see Figure S42 in the Supporting Information, Table 2) resembles that of $[1\text{-BF}_2][\text{BF}_4]$, with a slightly shorter B–B bond length of 1.709(4) Å, owing to the lower electronegativity of the chloride versus the fluoride ligands.

In solution and in the solid state at room temperature, isolated samples of $[1\text{-BCl}_2][\text{BCl}_4]$ converted overnight to a 1:1 mixture of the neutral $\text{sp}^2\text{-sp}^3$ diborane $(\text{CAAC})\text{BHCl}(\text{BCl}_2)$ (**2-Cl**: $\delta_{11\text{B}} = 75.8$ (br), -13.0 (br) ppm) and $(\text{Me}_3\text{P})\text{BCl}_3$ ($\delta_{11\text{B}} = 3.1$ (d, $J_{11\text{B}-31\text{P}} = 164$ Hz) ppm, Scheme 4d).^[38] The ^{11}B NMR shifts of **2-Cl** resemble those of the singly NHC-stabilized adducts of B_2Cl_4 ($\delta_{11\text{B}} = +69$, -5 ppm), which are formed at low temperature and decompose upon warming.^[39] Diborane **2-Cl** was also unstable both in solution and in the solid state, undergoing a B–B bond-cleaving intramolecular chloride migration to yield the known compound $(\text{CAAC})\text{BHCl}_2$, **3-Cl**,^[35] as the sole isolable product (Scheme 4e). The comparison of the ^{11}B and ^{31}P NMR spectra of $[1\text{-BCl}_2][\text{BCl}_4]$ and **2-Cl** with those of the complex product mixture first obtained upon reacting **1** with $(\text{Me}_2\text{S})\text{BBr}_3$

enabled the identification of $[1\text{-BBr}_2][\text{BBr}_4]$ ($\delta_{11\text{B}} = 74.5$ (br, BBr_2), -22.4 (br, BH), -23.2 (s, BBr_4) ppm; $\delta_{31\text{P}} = -9.9$ (m) ppm) and **2-Br** ($\delta_{11\text{B}} = 70.9$ (br, BBr_2), -9.0 (br, BH) ppm) as the major intermediates in the formation of **3-Br**. Overall, the 1:2 reactions of **1** with $(\text{Me}_2\text{S})\text{BCl}_3$ and $(\text{Me}_2\text{S})\text{BBr}_3$ thus result in the two-electron oxidation of **1** via one-electron oxidation intermediates.

The only other crystalline product that was consistently isolated from the reaction of **1** with $(\text{Me}_2\text{S})\text{BBr}_3$, albeit not in quantities sufficient for full characterization, was the unsymmetrical doubly base-stabilized diborane **4** ($\delta_{11\text{B}} = -4.8$ (BBr_2PMe_3) and -15.3 (BHBr) ppm; $\delta_{31\text{P}} = -11.7$ (m) ppm), which results from the phosphine-bromide rearrangement of **1-BBr₃** (Scheme 4f).^[40] The solid-state structure of **4** (Figure 8, Table 2) confirms the migration of the PMe_3 ligand to B2 and of one bromide to B1. The B–B bond length of 1.736(5) Å is significantly shorter than in **1-BCl₃** (1.784(4) Å). The phosphine and CAAC ligands are in an *anti* conformation, with a (P1–B2–B1–C1) torsion angle of $169.9(2)^\circ$. Compound **4**, which proved indefinitely stable at room temperature in solution, is the first structurally characterized example of a neutral (trihalo) hydrodiborane and a rare example of a neutral diborane stabilized by two different Lewis bases.^[41] It is structurally very similar to the carbene- and PMe_3 -stabilized tetrabromodiborane reported by Kinjo and co-workers.^[41b]

Finally, the 1:1 reaction of **1** with BI_3 in DFB proceeded very selectively, and independent of reaction temperature, to a single product displaying a broad ^{11}B NMR resonance at -28.3 ppm and a ^{31}P NMR multiplet at -14.3 ppm (Scheme 4g). After filtration from a small amount of intractable brown by-product,^[42] recrystallization yielded single crystals of the two-electron oxidation product $[1\text{-I}]\text{I}$ (Figure 8, Table 2). The fact that only one equivalent of BI_3 is required and the PMe_3 ligand remains bound to the boron center suggests a different reaction pathway from that of **1** with BBr_3 . Assuming that, here too, the Lewis adduct **1-BI₃** is formed first as an intermediate, the latter may be decomposing directly to $[1\text{-I}]\text{I}$ by iodide migration from B2 to B1 concomitant with B–B bond cleavage. Alternatively, the reaction may proceed via the one-electron oxidation intermediate $1^{*\cdot}$, with subsequent iodine abstraction to yield $[1\text{-I}]\text{I}$.

Computational analysis of B–E bonding in 1-EX₃

In order to gain a deeper understanding of the bonding situation in the borylene-EX₃ adducts, B–E bond dissociation energies (BDEs) for the isolated 1-ECl₃ adducts (E = B, Al, Ga, In) and the putative 1-BX₃ adducts (X = F, Br, I) were calculated at the BP86-D3BJ/TZ2P//PBEh-3c and the improved double hybrid RI-DSD-BLYP–D3BJ/def2-QZVPP//PBEh-3c levels of theory (see details in the Supporting Information). The calculated B–E bond lengths match those of the solid-state structures closely (within 1.5 to 2%), including B–Al being slightly longer than B–Ga (Tables 2 and 3). The B–E BDEs at both levels of theory show similar trends, notwithstanding the typical overbinding by the BP86 functional. The comparison of the B–B BDEs of the putative 1-BX₃ adducts with the B–E BDEs of the isolated 1-ECl₃ adducts shows that the former would theoretically be stable enough for isolation if subsequent halide abstraction and/or redox processes could be prevented. In line with the general trend in Lewis acidities of the boron trihalides,^[43] calculated B–B BDEs in 1-BX₃ nearly double between 1-BF₃ and 1-BCl₃, then increase more slowly upon descending the halide group further. The B–E BDEs of 1-ECl₃ increase substantially from BCl₃ to InCl₃, nearly doubling upon going from 1-BCl₃ and 1-AlCl₃, then increasing more slowly upon descending group 13 further. Energy decomposition analysis (EDA) shows that this trend goes back to substantially diminished preparation energies ΔE_{prep} (the energy necessary to deform the fragments from their individual equilibrium structures to the structures they assume in the respective adduct), whereas the corresponding interaction energies are essentially constant for all four 1-ECl₃ adducts. Deformation of the ECl₃ fragments in particular dominates ΔE_{prep} . While the structural deformation, as measured by the sum of angles about the group 13 atom, is almost identical in all four cases, the bending potentials flatten substantially from BCl₃ to InCl₃ (see Figure S43 in the Supporting Information). Furthermore, while B–B bonding in 1-BX₃ is dominated by orbital interactions (54–60%), the contribution of which increases upon descending the halide group, B–E bonding in 1-ECl₃ (E = Al, Ga, In) is dominated by electrostatic interactions (51–57%), the contribution of which increases upon descending group 13 (see Tables S4 and S5 in the Supporting Information). This is in line with the increasing polarization of the B–B bond in 1-BX₃ for the lighter halides and of the B–E bond in 1-ECl₃ for the heavier group 13 elements.

Conclusion

In this study we have shown that the (CAAC,PMe₃)-stabilized hydroborylene **1** offers an easily accessible, versatile platform for the systematic assessment of reactivity patterns of borylenes towards Lewis-acidic group 13 trihalides, EX₃. Depending on the nature of E and X the reactivity can be tuned either in favor of neutral Lewis adduct formation or one- and/or two-electron redox processes.

With all group 13 trichlorides the 1:1 reaction yields the corresponding Lewis adduct 1-ECl₃ (E = B, Al, Ga, In) as the major product. The proportion of the radical cation by-product 1^{•+}, resulting from the one-electron oxidation of **1** by ECl₃, increases upon descending group 13, as the corresponding reduction potential of ECl₃ becomes more positive. The influence of the halide in these reactions becomes apparent in the reactions of **1** with BF₃, BBr₃ and BI₃ sources. While it appears reasonable to assume initial formation of 1-BX₃ adducts, these species are too reactive to isolate. For X = F, fluoride abstraction by a second equivalent BF₃ is significantly more rapid than 1-BF₃ adduct formation, leading to the stable borylboronium species [1-BF₂][BF₄]. For X = Br, 1-BBr₃ also converts instantly to [1-BBr₂][BBr₄] which is, however, highly unstable towards intramolecular ligand exchange and redox processes, ultimately resulting in the two-electron oxidation of **1**. Finally, for X = I, only the product of the two-electron redox reaction between **1** and BI₃ is observed, thereby confirming the trend for increased redox processes down the group, as the B–X bond weakens.^[44]

Based on the calculated BDEs, **1** acts as a typical strong Lewis base towards BX₃. For the adducts of **1** with ECl₃ the B–E BDEs increase down the group owing to successively weaker bending potentials of the ECl₃ groups, which facilitates geometric distortion in the course of adduct formation.

Beyond the fundamental interest in the reactivity patterns of a Lewis-basic borylene towards group 13 Lewis acids, and the study of borylene-group 13 Lewis adduct bond enthalpies, the 1:2 reaction of **1** and BCl₃ also provides a novel synthetic route towards an otherwise inaccessible, electron-precise, unsymmetrical diborane, 2-Cl. Such species have become highly sought after as they display an intrinsic polarization of the B–B bond,^[45] making them significantly more reactive than commercially available symmetrical diboron reagents, in particular for uncatalyzed borylation and diboration reactions.^[46] Furthermore, the presence of halide substituents in the cationic

Table 3. Bond dissociation, preparation and interaction energies according to energy decomposition analysis and B–E bond lengths for the 1-EX₃ adducts.

Sample	BDE ^[a]	BDE ^[b]	$\Delta E_{\text{int}}^{\text{[b]}}$ [kcal mol ⁻¹]	$\Delta E_{\text{prep}}^{\text{[b]}}$ [kcal mol ⁻¹]	B–E [Å] ^[b]
1-BCl ₃	21.8	27.5	–97.9	68.5	1.81
1-AlCl ₃	40.7	48.4	–91.2	39.6	2.23
1-GaCl ₃	48.8	54.0	–97.7	42.5	2.19
1-InCl ₃	56.4	61.8	–98.6	33.8	2.36
1-BF ₃	11.3	16.1	–72.5	53.8	1.89
1-BBr ₃	27.8	34.3	–108.3	70.6	1.81
1-BI ₃	31.0	45.3	–122.0	73.6	1.81

[a] Based on improved RI-DSD-BLYP–D3BJ/def2-QZVPP//PBEh-3c calculations. [b] BP86-D3BJ/TZ2P//PBEh-3c.

borylboronium species, $[1-BX_2]^+$, provides a potential handle either for subsequent ligand exchange by salt metathesis or for subsequent reduction chemistry.

Experimental Section

Crystallographic data: Deposition Numbers 2107378 ([1][BAR^F₄]), 2107379 ([1-BCl₃][BCl₄]), 2107380 (1), 2107381 (1-AlCl₃), 2107382 ([1-BF₂][BF₄]), 2107383 ([1-I]), 2107384 (1-InCl₃-CHCl₃), 2107385 (1-BCl₃-C₆H₄F₂), 2107386 (4), 2107387 (1-InCl₃-C₆H₄F₂), 2107388 (1-GaCl₃), 2107389 ([1-H][In₂Cl₆]) and 2107390 (1-BCl₃-C₆H₆) contain the supplementary crystallographic data for this paper. These data are provided free of charge by the joint Cambridge Crystallographic Data Center and Fachinformationszentrum Karlsruhe Access Structures service.

Acknowledgements

Funding from the Deutsche Forschungsgemeinschaft is gratefully acknowledged. Quantum-chemical computations were performed at the Center for Scientific Computing (CSC) Frankfurt on the Goethe and Fuchs high-performance computer clusters. Open Access funding enabled and organized by Projekt DEAL.

Conflict of Interest

The authors declare no conflict of interest.

Keywords: bond dissociation energies · borylene · group 13 · Lewis adducts · redox processes

- Y. Segawa, M. Yamashita, K. Nozaki, *Science* **2006**, *314*, 113–115.
- R. Kinjo, B. Donnadiou, M. Ali Celik, G. Frenking, G. Bertrand, *Science* **2011**, *333*, 610–613.
- a) M. Soleihavoup, G. Bertrand, *Chem* **2020**, *6*, 1275–1282; b) M.-A. Légaré, C. Prankevicus, H. Braunschweig, *Chem. Rev.* **2019**, *119*, 8231–8261; c) M. Soleihavoup, G. Bertrand, *Angew. Chem. Int. Ed.* **2017**, *56*, 10282–10292; *Angew. Chem.* **2017**, *129*, 10416–10426; d) M. Yamashita, *Bull. Chem. Soc. Jpn.* **2011**, *84*, 983–999; e) M. Yamashita, K. Nozaki, *Bull. Chem. Soc. Jpn.* **2008**, *81*, 1377–1392.
- K. Nozaki, Y. Aramaki, M. Yamashita, S.-H. Ueng, M. Malacria, E. Lacôte, D. P. Curran, *J. Am. Chem. Soc.* **2010**, *132*, 11449–11451.
- N. Dettenrieder, C. Schädle, C. Maichle-Mössmer, R. Anwänder, *Dalton Trans.* **2014**, *43*, 15760–15770.
- a) N. Dettenrieder, C. Schädle, C. Maichle-Mössmer, P. Sirsch, R. Anwänder, *J. Am. Chem. Soc.* **2014**, *136*, 886–889; b) N. Dettenrieder, H. M. Dietrich, C. Schädle, C. Maichle-Mössmer, K. W. Törnroos, R. Anwänder, *Angew. Chem. Int. Ed.* **2012**, *51*, 4461–4465; *Angew. Chem.* **2012**, *124*, 4537–4541.
- D. Dange, C. P. Sindlinger, S. Aldridge, C. Jones, *Chem. Commun.* **2017**, *53*, 149–152.
- a) A. V. Protchenko, D. Dange, J. R. Harmer, C. Y. Tang, A. D. Schwarz, M. J. Kelly, N. Phillips, R. Tirfoin, K. H. Birjumar, C. Jones, N. Kaltsoyannis, P. Mountford, S. Aldridge, *Nat. Chem.* **2014**, *6*, 315–319; b) Y. Hayashi, Y. Segawa, M. Yamashita, K. Nozaki, *Chem. Commun.* **2011**, *47*, 5888–5890.
- A. Yagi, H. Kisu, M. Yamashita, *Dalton Trans.* **2019**, *48*, 5496–5499.
- H. Braunschweig, R. D. Dewhurst, L. Pentecost, K. Radacki, A. Vargas, Q. Ye, *Angew. Chem. Int. Ed.* **2016**, *55*, 436–440; *Angew. Chem.* **2016**, *128*, 447–451.
- L. Kong, W. Lu, L. Yongxin, R. Ganguly, R. Kinjo, *Inorg. Chem.* **2017**, *56*, 5586–5593.
- M. Arrowsmith, D. Auerhammer, R. Bertermann, H. Braunschweig, G. Bringmann, M. A. Celik, R. D. Dewhurst, M. Finze, M. Grüne, M. Hailmann, T. Hertle, I. Krummenacher, *Angew. Chem. Int. Ed.* **2016**, *55*, 14464–14468; *Angew. Chem.* **2016**, *128*, 14680–14684.
- M. Arrowsmith, J. I. Schweizer, M. Heinz, M. Härterich, I. Krummenacher, M. C. Holthausen, H. Braunschweig, *Chem. Sci.* **2019**, *10*, 5095–5103.
- a) D. A. Ruiz, M. Melaimi, G. Sherbrand, *Chem. Commun.* **2014**, *50*, 7837–7839; b) J. Böhnke, M. Arrowsmith, H. Braunschweig, *J. Am. Chem. Soc.* **2018**, *140*, 10368–10373.
- The 1:1 reaction of **1** with (Me₂S)BCl₃ was more selective for the formation of 1-BCl₃ than the reaction with BCl₃ (1 M in hexane).
- (Me₂S)BCl₃: a) M. J. Bula, J. S. Hartman, *J. Chem. Soc. Dalton Trans.* **1973**, 1047–1054; (Me₂O)BCl₃: b) D. E. Young, G. E. McAchran, S. G. Shore, *J. Am. Chem. Soc.* **1966**, *88*, 4390–4396; (Et₂O)BCl₃: c) T. P. Onak, H. Landesman, R. E. Williams, I. Shapiro, *J. Phys. Chem.* **1959**, *63*, 1533–1535; (Me₃N)BCl₃: d) H. Nöth, H. Vahrenkamp, *Chem. Ber.* **1966**, *99*, 1049–1067; (Me₂PhN)BCl₃: e) A. Del Grosso, M. D. Helm, S. A. Solomon, D. Caras-Quintero, M. J. Ingleson, *Chem. Commun.* **2011**, *47*, 12459–12461 <; (tBu₂HP=O)BCl₃: f) Dornhaus, S. Scholz, I. Sängler, M. Bolte, M. Wagner, H.-W. Lerner, *Z. Anorg. Allg. Chem.* **2009**, *635*, 2263–2272; (R₃P)BCl₃: f) R. B. Coapes, F. E. S. Souza, M. A. Fox, A. S. Batsanov, A. E. Goeta, D. S. Yufit, M. A. Leech, J. A. K. Howard, A. J. Scott, W. Clegg, T. B. Marder, *J. Chem. Soc. Dalton Trans.* **2001**, 1201–1209; (CAAC)BCl₃: g) M. Arrowsmith, J. I. Schweizer, M. Heinz, M. Härterich, I. Krummenacher, M. C. Holthausen, H. Braunschweig, *Chem. Sci.* **2019**, *10*, 5095–5103; (SIDip)BCl₃: h) G. Kundu, S. Pahar, S. Tothadi, S. S. Sen, *Organometallics* **2020**, *39*, 4696–4703.
- S. Hagspiel, M. Arrowsmith, F. Fantuzzi, A. Hermann, V. Paprocki, R. Drescher, I. Krummenacher, H. Braunschweig, *Chem. Sci.* **2020**, *11*, 551–555.
- R. Benn, E. Janssen, H. Lemkuhl, A. Rufinska, *J. Organomet. Chem.* **1987**, *333*, 155–168.
- 1-GaCl₃** and **1-InCl₃** were easily isolated as they readily crystallized overnight from the respective reaction mixture, the first after filtration and storage at –30 °C, the second at room temperature. Unlike **1-BCl₃** and **1-AlCl₃**, **1-GaCl₃** and **1-InCl₃** were stable in CDCl₃, whereby the solubility of **1-InCl₃** was too low (< 1 mg mL⁻¹) to acquire meaningful ¹H or ¹³C{¹H} NMR data.
- [**1-H**]⁺ was formed in 5–25% in the 1:1 reaction with GaCl₃, in 30–50% in the 1:1 reaction with InCl₃.
- Crystals obtained from the third crystallization fraction at –30 °C.
- The proportion of [**1**]⁺ generated in these reactions was observed to increase upon descending the group and at higher reaction temperatures.
- N. G. Connelly, W. E. Geiger, *Chem. Rev.* **1996**, *96*, 877–910.
- a) M. Arrowsmith, D. Auerhammer, R. Bertermann, H. Braunschweig, M. A. Celik, J. Erdmannsdörfer, T. Kupfer, I. Krummenacher, *Angew. Chem. Int. Ed.* **2017**, *56*, 11263–11267; *Angew. Chem.* **2017**, *129*, 11417–11421; b) P. Bissinger, H. Braunschweig, A. Damme, C. Hörl, I. Krummenacher, T. Kupfer, *Angew. Chem. Int. Ed.* **2015**, *54*, 359–362; *Angew. Chem.* **2015**, *127*, 366–369; c) H. Braunschweig, P. Bissinger, A. Damme, T. Kupfer, I. Krummenacher, A. Vargas, *Angew. Chem. Int. Ed.* **2014**, *53*, 5689–5693; *Angew. Chem.* **2014**, *126*, 5797–5801.
- The one-electron oxidation of **1** with [Fc][BAR^F₄]⁺ also yielded [**1**][BAR^F₄]⁺, the latter then effecting a radical hydrogen abstraction at the ferrocene by-product to yield [**1-H**][BAR^F₄]⁺ and [**1-Fc**][BAR^F₄]⁺, which is why [Cp*₂Fe][BAR^F₄]⁺ had to be employed.
- S. Kundu, S. Sinhababu, V. Chandrasekhar, H. W. Roesky, *Chem. Sci.* **2019**, *10*, 4727–4741.
- T. E. Stennett, R. Bertermann, H. Braunschweig, *Angew. Chem. Int. Ed.* **2018**, *57*, 15896–15901; *Angew. Chem.* **2018**, *130*, 16123–16128.
- A. Hofmann, C. Prankevicus, T. Tröster, H. Braunschweig, *Angew. Chem. Int. Ed.* **2019**, *58*, 3625–3629; *Angew. Chem.* **2019**, *131*, 3664–3668.
- B. Cordero, V. Gómez, A. E. Platero-Prats, M. Revés, J. Echeverría, E. Cremades, F. Barragán, S. Alvarez, *Dalton Trans.* **2008**, 2832–2838.
- Solvents tried: DFB, toluene, benzene, hexane. At temperatures below 0 °C no reaction was observed.
- a) J. A. Plumbley, J. D. Evanseck, *J. Phys. Chem. A* **2009**, *113*, 5985–5992; b) F. Bessac, G. Frenking, *Inorg. Chem.* **2003**, *42*, 7990–7994; c) G. Frenking, S. Fau, C. M. Marchand, H. Grützmacher, *J. Am. Chem. Soc.* **1997**, *119*, 6648–6655; d) J. F. Liebman, *Struct. Chem.* **1990**, *1*, 395–397.
- P. Erdmann, J. Leitner, J. Schwarz, L. Greb, *ChemPhysChem* **2020**, *21*, 987–994.

- [33] There are two crystallographically distinct units of [1-BF₂][BF₄] in the asymmetric unit.
- [34] a) J. Cid, A. Hermann, J. E. Radcliffe, L. D. Curless, H. Braunschweig, M. J. Ingleson, *Organometallics* **2018**, *37*, 1992–1998; b) J. Zheng, Z. H. Li, H. Wang, *Chem. Sci.* **2018**, *9*, 1433–1438.
- [35] Reaction conditions tried: toluene, 1:1 DFB/toluene or hexane, –70 °C and –40 °C to rt; benzene, 1:1 benzene/hexane, hexane or DFB, rt.
- [36] According to ¹¹B and ³¹P NMR and EPR spectra the reaction mixture in 1:1 DFB/toluene after 10 min at –70 °C contained unreacted **1**, [1]^{•+}, [1-H][BBr₄], 1-BBr₃, **4** and [1-BBr₂][BBr₄].
- [37] M. Arrowsmith, J. D. Mattock, J. Böhnke, I. Krummenacher, A. Vargas, H. Braunschweig, *Chem. Commun.* **2018**, *54*, 4669–4672.
- [38] 2-Cl and (Me₃P)BCl₃ could be separated by fractional crystallization of the latter from a 1:10 DFB/hexanes mixture at –30 °C. Compound 2-Cl, however, could not be fully characterized due to its slow decomposition in solution and in the solid state.
- [39] L. Englert, A. Stoy, M. Arrowsmith, J. H. Müssig, M. Thaler, A. Deißberger, A. Häfner, J. Böhnke, F. Hupp, J. Seufert, J. Mies, A. Damme, T. Dellermann, K. Hammond, T. Kupfer, K. Radacki, T. Thiess, H. Braunschweig, *Chem. Eur. J.* **2019**, *25*, 8612–8622.
- [40] Multiple repeats of the 1:2 reaction between **1** and (Me₂S)BBr₃ only ever yielded a few crystals (<1 mg) of **4**, thus precluding full characterization. The phosphine-bromide rearrangement of 1-BBr₃ to **4** was observed by monitoring a reaction mixture of **1** and 0.8 equiv. BBr₃ in a 1:1 DFB/toluene solution at –30 °C for 3 hours.
- [41] a) T. E. Stennett, J. D. Mattock, I. Vollert, A. Vargas, H. Braunschweig, *Angew. Chem. Int. Ed.* **2018**, *57*, 4098–4102; *Angew. Chem.* **2018**, *130*, 4162–4167; b) W. Lu, Y. Li, R. Ganguly, R. Kinjo, *Angew. Chem. Int. Ed.* **2017**, *56*, 9829–9832; *Angew. Chem.* **2017**, *129*, 9961–9964; c) W. Lu, Y. Li, R. Ganguly, R. Kinjo, *J. Am. Chem. Soc.* **2017**, *139*, 5047–5050.
- [42] This is likely to be the polymerized by-product "BI".
- [43] a) A. R. Jupp, T. C. Johnstone, D. W. Stephan, *Inorg. Chem.* **2018**, *57*, 23, 14764–14771; b) P. Erdmann, L. Greb, *ChemPhysChem* **2021**, *22*, 935–943.
- [44] Y. R. Luo, *Comprehensive handbook of chemical bond energies*. Boca Raton: CRC Press **2007**.
- [45] a) R. D. Dewhurst, E. C. Neeve, H. Braunschweig, T. B. Marder, *Chem. Commun.* **2015**, *51*, 9594–9607; b) S. Pietsch, E. C. Neeve, D. C. Apperley, R. Bertermann, F. Mo, D. Qiu, M. S. Cheung, L. Dang, J. Wang, U. Radius, Z. Lin, C. Kleeberg, T. B. Marder, *Chem. Eur. J.* **2015**, *21*, 7082–7098; c) H. Braunschweig, A. Damme, R. D. Dewhurst, T. Kramer, T. Kupfer, K. Radacki, E. Siedler, A. Trumpp, K. Wagner, C. Werner, *J. Am. Chem. Soc.* **2013**, *135*, 8702–8707; d) Kleeberg, A. G. Crawford, A. S. Batsanov, P. Hodgkinson, D. C. Apperley, M. S. Cheung, Z. Lin, T. B. Marder, *J. Org. Chem.* **2012**, *77*, 785–789.
- [46] a) Z. Kuang, K. Yang, Y. Zhou, Q. Song, *Chem. Commun.* **2020**, *56*, 6469–6479; b) S. Ding, L. Xu, Z. Miao, *Molecules* **2019**, *24*, 1325; c) A. B. Cuenca, R. Shishido, H. Ito, E. Fernández, *Chem. Soc. Rev.* **2017**, *46*, 415–430; d) F. Zhao, X. Jia, P. Li, J. Zhao, Y. Zhou, J. Wang, H. Liu, *Org. Chem. Front.* **2017**, *4*, 2235–2255; e) E. C. Neeve, S. J. Geier, I. A. I. Mkhaliid, S. A. Westcott, T. B. Marder, *Chem. Rev.* **2016**, *116*, 9091–9161.

Manuscript received: September 8, 2021

Accepted manuscript online: October 1, 2021

Version of record online: November 11, 2021